ORIGINAL PAPER

The efficiency of nanolime and dibasic ammonium phosphate in the consolidation of beige limestone from the Pasargadae World Heritage Site

Atefeh Shekofteh[1] · Eduardo Molina[2,3] · Lucía Rueda-Quero[4] · Anna Arizzi[5] · Giuseppe Cultrone[5]

Abstract

The limestone used at the Pasargadae World Heritage Site in Iran, an outstanding open-air architectural heritage site dating from the Achaemenid period (sixth century BC), has suffered weathering due to interaction with the environment. It was built out of beige limestone that today shows scaling and pitting decay patterns. Two inorganic consolidating products that are very promising: nanolime and dibasic ammonium phosphate (DAP) were considered for the consolidation of the limestone. Consolidation treatments were conducted on samples from a quarry and applied using a paintbrush with 50% nanolime dispersion in isopropyl alcohol and 1.0 M DAP water solution. Superficial consolidation was evaluated by means of a micro-drilling resistance test, and color changes were assessed by spectrophotometry. The microstructure of the treated samples was observed using FE-SEM. The efficacy of the two consolidation treatments was also assessed by testing their hydric properties and durability (hydric tests, freeze-thaw, and salt crystallization cycles). The compactness in the altered samples was monitored by measuring the ultrasound propagation velocity. We found that the superficial resistance increased in a similar way with both treatments. However, spectrophotometry revealed a yellowish color in the samples treated with DAP. During FE-SEM observations, some diffused microcracks were detected on the surface of DAP treatment. When subjected to accelerated aging tests, both treatments managed to postpone the formation of the first microcrack during the freeze-thaw test and both showed outstanding stability during salt crystallization cycles. In conclusion, the nanolime product seems to be more compatible with beige limestone because it does not affect its aesthetic qualities (color, lightness, and a homogeneous layer formed on the surface of the stone). Moreover, previous research found that lime has a low propensity for biological growth. This supports its use as a consolidating product for the stone used in open-air archeological sites that are prone to microbial growth, such as the beige stone used in the Pasargadae WHS.

Keywords Inorganic Consolidant · Nanolime · DAP · HAP · Limestone consolidation · Pasargadae

✉ Atefeh Shekofteh
    shekofte.as@gmail.com

1   Department of Conservation of Cultural and Historical Properties, Faculty of Conservation, Art University of Isfahan, Isfahan 1744, Iran

2   Departamento de Ingeniería Estructural y Geotécnica, Escuela de Ingeniería, Pontificia Universidad Católica de Chile, Santiago, Chile

3   Centro de Excelencia en Geotermia de Los Andes (Cega, Fondap-Conicyt), Universidad de Chile, Santiago, Chile

4   Department of Sculpture, University of Granada, Granada, Spain

5   Department of Mineralogy and Petrology, Faculty of Science, University of Granada, Granada, Spain

Introduction

This research is based on morphological, physical, and durability tests carried out on the beige stone used at the Pasargadae World Heritage Site (WHS), an archeological site located in Fars province in southern Iran. Pasargadae WHS was the capital of the Achaemenid Empire (559–330 BC) (Boardman 2000; Stronach 1985) and includes some important architectural remains such as three palaces and, in particular, the tomb of *Cyrus the Great*. This led the site to be added to the UNESCO World Heritage list in 2004. A detailed characterization and damage assessment of the stones used at Pasargadae has already been carried out by Shekofteh et al.

(2018) and Shekofteh el al. (2016), who found that the beige stones were pure limestone and that less common dolostones were also present. Almost all the beige stone blocks show decay in the form of scaling, peeling, and pitting (Fig. 1), caused mostly by microorganism attack (pitting and peeling) and temperature fluctuations or frost (scaling). In particular, microbial growth is considered the most problematic issue for the durability of the beige stone (Shekofteh 2018). The microorganisms, such as fungi and lichens, typically found at Pasargadae WHS, were studied by Mohammadi and Maghboli-Balasjin (2014) and Sohrabi et al. (2017).

Due to the decay affecting the surface of the beige stone used at the Pasargadae WHS, it is necessary to carry out specific consolidation treatments in situ, so as to prevent worse damage to the stone and further alteration due to environmental weathering factors. Consolidation can help preserve historical monuments by positively modifying the pore network and physical properties of the treated substrate so as to reduce further deterioration (Wheeler and Goins 2005). However, an inappropriate treatment can accelerate the decay of the materials. It is therefore important to choose the right product for the material being treated. In consolidation treatments today, the compatibility of the consolidant with the substrate is as important as the principle of reversibility (which was often

a more idealistic than realistic constraint) (van Hees et al. 2014; Graziani et al. 2015). It is therefore fundamental to ensure the compatibility of the consolidating treatment (Delgado Rodrigues 2001; Price and Doehne 2011). Consolidation treatments should also meet two further requirements: effectiveness and durability (Hansen et al. 2003). A compatible consolidation treatment can improve both the mechanical properties and the durability of the material. For these reasons, careful planning and preliminary testing are required to ensure that the right consolidating product is selected and that it is applied in the most effective way.

The aim of this study is to find a suitable consolidating product to prevent the peeling and scaling of the beige stone from the Pasargadae WHS, increasing its superficial strength by preliminary examination, and comparing the effectiveness of two of the most recently used inorganic materials: nanolime and dibasic ammonium phosphate.

Organic consolidating products such as acrylics and epoxy resins are easy to apply, flexible, and show good adhesion to the substrate. Unfortunately, they are often incompatible with the substrate in physicochemical terms (Borsoi et al. 2012; Carretti and Dei 2004). In addition, the long-term effectiveness of these resins is impaired by the direct action of sunlight, which promotes oxidation reactions (Chiantore and Lazzari
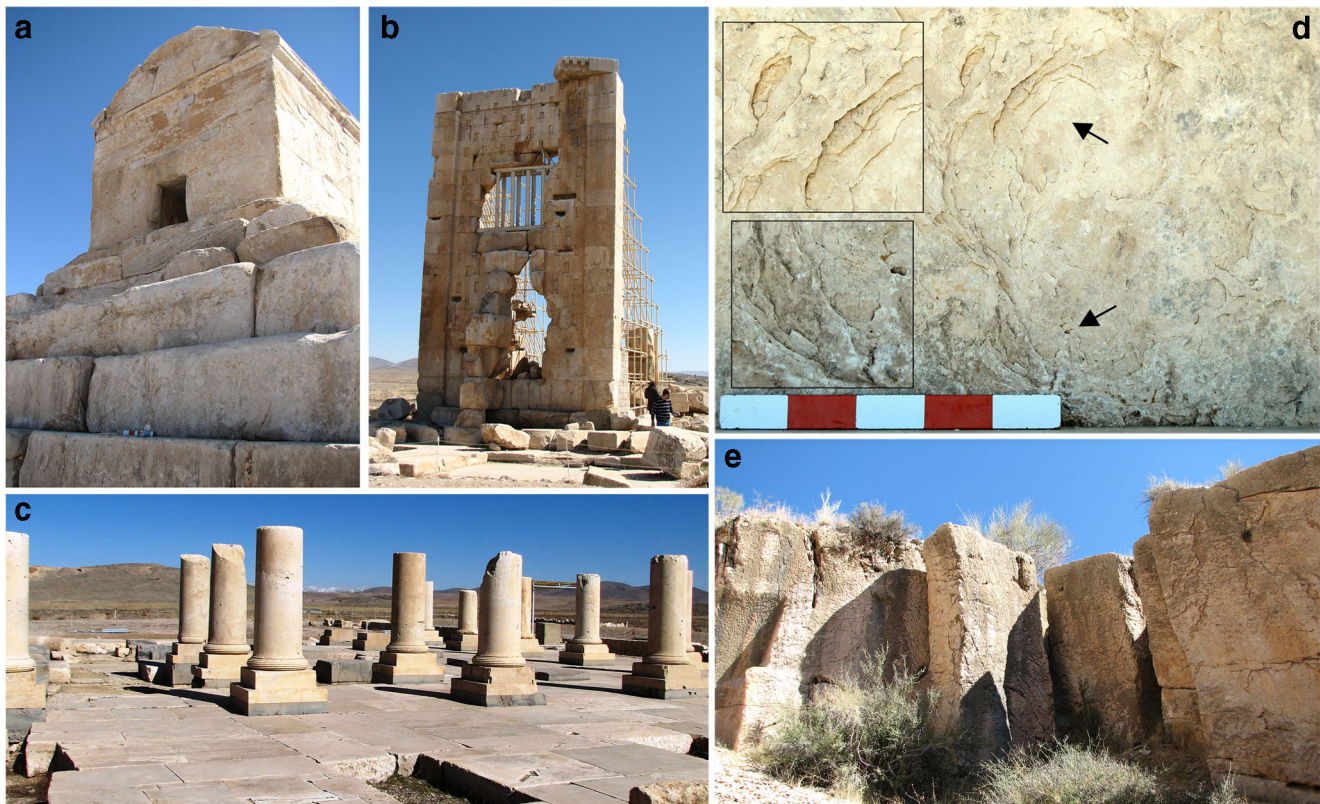

Fig. 1 Architectural remains at the Pasargadae WHS. **a** Tomb of *Cyrus the Great*. **b** *Zendān-e Soleymān* tower. **c** Residential palace. **d** Scaling decay pattern on the beige stone from a step in *Cyrus* tomb, the black arrows show the location of the magnified insets which indicate scaling, possibly caused by frost. **e** "Almas-bori"—an ancient quarry believed to be the source of the beige stones used at the Pasargadae WHS

2001). The alkoxysilane consolidating products (the most common products used by conservators) also have certain drawbacks such as their tendency to crack and stone substrate-gel incompatibilities (Zornoza-Indart et al. 2017). Given the importance of the chemical compatibility requirement, we chose two inorganic materials, both of which are considered very promising (Graziani et al. 2017a; Possenti et al. 2016; Sassoni et al. 2016; Borsoi et al. 2017; Sierra-Fernandez et al. 2018; Borsoi et al. 2016a): nanolime and dibasic ammonium phosphate (DAP (NH$_4$)2HPO$_4$). The application of lime (e.g., in the form of limewater) is recommended due to its potential as a consolidating product in calcareous materials. It leads to the deposition of interlocking calcium carbonate crystals, but this may have limited consolidating effect if the crystals are deposited too superficially due to the limited solubility of Ca(OH)$_2$ in water (Hansen et al. 2003; Tiano 1995; Fidler 2002; Rodriguez-Navarro et al. 2013). Nanolimes, however, are colloidal alcoholic dispersions of calcium hydroxide nanoparticles with a spherical to hexagonal shape that show high reactivity when in high concentration (Dei and Salvadori 2006; Ambrosi et al. 2001). In the last decade, nanolime technology is replacing the traditional lime application technique because its nanoscale calcium hydroxide particles and higher calcium hydroxide concentration in alcohol solvent allow deeper penetration into the substrate (Giorgi et al. 2000; Natali et al. 2014). Nanolime consolidant is mainly recommended for recovering the cohesion of the surface, but has proved ineffective in the consolidation of limestone suffering from deep decay (Borsoi et al. 2016b). Given the specific decay patterns shown by the beige stone (e. g., scaling, peeling, and pitting on the surface), a nanolime consolidant could be an appropriate consolidating material due to its compatibility with limestone and its ability to consolidate the surface.

According to the so-called hydroxyapatite or HAP method, initially proposed in 2011 for the conservation of carbonate stones (Sassoni et al. 2011; Matteini 2008; Sassoni et al. 2018), dibasic ammonium phosphate (DAP) in an aqueous solution reacts with the carbonate substrate forming CaP, ideally hydroxyapatite (HAP -Ca$_5$(PO$_4$)$_3$(OH)-) (the most stable CaP at pH> 4). The HAP method is known to protect minerals against weathering, because HAP has a much lower solubility and dissolution rate than calcite and because its lattice parameters match well with calcite (Hansen et al. 2003; Sassoni et al., 2018). Although HAP is the most desirable phase formed by this reaction, other CaP phases may also form (such as octacalcium phosphate, calcium-deficient HAP, dicalcium phosphate anhydrous, amorphous calcium phosphate). Although these phases are more soluble than HAP, they are still less soluble than calcite and ensure better application of the consolidant which covers the surface more evenly and completely (Naidu and Scherer 2014). Moreover, the calcium phosphate formed in this way has been found to improve the mechanical properties of weathered limestone by re-establishing cohesion among calcite grains (Matteini et al. 2011). In fact, a low concentration of DAP solution has low viscosity and can penetrate deeply into weathered limestone (> 25 mm) (Sassoni et al. 2018). In addition, these calcium phosphates do not significantly alter the porosity and pore size distribution of the substrate and make it hydrophobic, thus enabling re-treatment in possible future interventions (Graziani et al. 2015). As DAP has been shown to be effective at improving the cohesion among grains and, in some cases, the hydric properties of calcareous stones, we thought that DAP could be an appropriate consolidating material to reduce further decay (mainly surface issues such as peeling) in the beige stone from the Pasargadae open-air WHS.

Materials and methods

Stone base material

The beige stone used in this work was collected from "Almasbori," an ancient quarry (Fig. 1) believed to date from the Achaemenid period (Tilia 1968). Analysis of the stones from this quarry indicated that they had a similar composition to the original stones from Pasargadae (Shekofteh 2018). Samples were cut into cubes measuring $40 \times 40 \times 40$ mm^3, and only 3 samples were prepared per test due to the limits on sampling from this ancient quarry. During the experiments, we did not consider the orientation of the stone fabric because the stone blocks used in Pasargadae WHS were not positioned according to their orientation. This is demonstrated by the fact that blocks with different orientations are sometimes located adjacent to one another or in the same row.

Consolidation methods

Given that nanolime transport is strictly related to the properties of the solvent and that the alcoholic solvent guarantees a stable dispersion which allows efficient deep penetration of the materials (Natali et al. 2014), we chose Nanorestore®, C. T. S.; Ca(OH)$_2$ colloidal dispersion (nanolime) in isopropyl alcohol (1:1 proportion) with a particle size ≤ 100 nm. We also considered that this product could be appropriate as it has already proved to be efficient at reducing stone porosity and water absorption ability, while increasing its superficial drilling resistance in comparison with other similar products (Otero et al. 2018). NL (nanolime) was applied using a paintbrush. We opted for this method rather than other possible application methods because it ensures a continuous supply of fluid to the stone and it is easy to control, even in situ. This is why the paintbrush is the most widely used method for consolidant application in the field (Franzoni et al. 2015a; Franzoni et al. 2015b). Before applying NL, ultrasonic

dispersion was performed by placing the products in an ultrasonic bath for 5 min in order to prevent agglomeration of the nanoparticles. The six faces of the cube samples were impregnated with a brush with a gap of 30 min between each stroke until the surface was fully saturated, as advised by the manufacturer and due to its high reactivity when in high concentration (Dei and Salvadori 2006) (this procedure was repeated 8 times). After application of the consolidant, the samples were wrapped in a water-impregnated cellulose pulp poultice for 1 h to increase the penetration depth by reducing the evaporation rate, as advised by experts. The samples were then unwrapped and left under laboratory conditions (25 ± 5 °C T, 45 ± 5% RH). In order to enhance the carbonation of the $Ca(OH)_2$ nanoparticles thereby strengthening the consolidating effect on the treated substrates (López-Arce et al. 2011; Daniele et al. 2008), deionized water was sprayed on each face of the samples once every 24 h for 1 week.

As regards the treatment with dibasic ammonium phosphate (DAP), dispersions with concentrations ranging from 0.1 to 3.7 M (the latter corresponding to the saturation concentration at room temperature (Sassoni et al. 2018)) had been initially taken into consideration for this study. Finally, a DAP (Sigma-Aldrich company) 1.0 M with an aqueous solution with no further reduction in concentration was chosen, in order to apply it easily in situ. In fact, according to the literature, high concentration usually led to cracking in the consolidation layer (Dei and Salvadori 2006; Graziani et al. 2016) and low concentration has been recommended to reduce cracking of CaP coating (Sassoni et al. 2018). The six faces of cube samples were treated with DAP in 2 brush strokes. This is because we thought that more than 2 brush strokes would cause an accumulation of DAP on the surface during the test and because DAP is normally applied with very few brush strokes in order to reduce cracking. The samples were then left wrapped in plastic film for 24 h to prevent evaporation. One potential problem with DAP treatment is that unreacted DAP may remain inside the stone at the end of the treatment. This could favor biological growth due to the presence of phosphorus and nitrogen in unreacted DAP (Song et al. 2002; Barriuso et al. 2017). To avoid this, the treated surface was rinsed twice at 24 h intervals, so as to eliminate any unreacted DAP from the surface and from inside the pores. The samples were stored for 8 days under laboratory conditions before the tests.

Assessment of the consolidation procedure

Free water absorption and drying

The results of consolidant efficiency and durability tests must be interpreted in relation to all the aspects and factors that cause decay. The study of the hydric properties of stones is fundamental for the evaluation of their durability, since water is one of the main sources of decay, as has happened with the stones from the Pasargadae site (Shekofteh et al. 2018). The water absorption test was carried out according to the UNE-EN 13755 (2008). Samples were oven-dried at 60 °C for 24 h before the test. Free water absorption (A_b) was measured as follows at atmospheric pressure:

$$A_b = \frac{M_1 - M_0}{M_0} \times 100,$$

Where M_1 is the mass of the sample saturated with water at atmospheric pressure (until constant mass is reached) and M_0 is the mass of the dried sample (in g).

The water drying test was performed according to the Normal 29/88 (1988) on the same samples at the end of the free water absorption test. The rate of drying was calculated by measuring the decrease in the mass of the samples due to water loss over time. The drying index (D_i) was measured using the following equation:

$$D_i = \frac{\int_{t_0}^{t_f} F(M_t) dt}{M_s \times t_f},$$

Where M_t represents a decreasing water weight content as a function of time, M_s (in g) is the saturated mass and t_f (in min) is the end time of the test.

Porosity and densities

In order to obtain information on the pore system of the stone, we followed the UNE-EN 1936 (2007) to determine the open porosity (P_{HT}) and the bulk (ρ_{Hb}) and the skeletal (ρ_{Hsk}) densities as follows:

$$P_{HT} = \frac{M_s - M_0}{M_s - M_H} \times 100;$$

$$\rho_{Hb} = \frac{M_0}{M_s - M_H};$$

$$\rho_{Hsk} = \frac{M_0}{M_s - M_H},$$

where M_S is the mass of the sample saturated with water under vacuum and M_H is the mass of the sample saturated with water under vacuum and weighed in water (in g).

Water absorption by capillary uptake

The capillary uptake test was performed according to the UNE-EN 1925 (2000). The capillarity coefficient (C_c) of the same samples before and after consolidation was obtained by measuring the slope of the initial straight line of the capillarity water absorption curves:

$$C_c = \frac{M_t - M_0}{A\sqrt{t}},$$

Where M_t is the amount of water absorbed at time t (in min) and A (in m^2) is the area of the sample in contact with water.

Water vapor permeability

The water vapor permeability of a material is a measure of the capacity of water vapor to pass through it. This capacity allows the stone to "breathe" (to dry out quickly), thus preventing water from being trapped beneath the surface and reducing damage due to freeze-thaw and salt crystallization phenomena. The vapor permeability coefficient (K_v) was measured following the UNE-EN 15803 (2010) on the same samples before and after consolidation treatment. Three samples per each material ($10 \times 40 \times 40$ mm in size) were kept under the same conditions ($T = 23 \pm 1$ °C, RH = 50%), until a constant mass was reached. Then, the whole mass was measured once every 24 h for 12 days under the same controlled temperature and RH conditions, and a linear trend curve was obtained from the decrease in mass over time. The vapor permeability coefficient (K_v g/m^{2}h) was calculated using the following equation:

$$K_v = \frac{\Delta M / A}{t}$$

where ΔM is the amount of water vapor transfer at time (t in s), and A (in mm^2) is the exposed surface area of samples 10-mm thick.

Accelerated aging tests

Freeze-thaw and salt crystallization tests were selected as the most representative aging tests. The freeze-thaw test is particularly appropriate for the Pasargadae site, given the evidence of frost damage on the stones and the frequent below-zero temperatures (Shekofteh et al. 2018). Even though we did not find any evidence of salt decay on the stones from the Pasargadae WHS, we decided to carry out the salt crystallization test because the results can help us assess the effectiveness of the consolidating products at protecting the stone. The changes caused by the freeze-thaw test were controlled by measuring the weight (wt%) during each cycle according to the UNE-EN 12371 (2011) and the damage caused by salt crystallization was assessed according to the UNE-EN 12370 (2001). The edges were painted prior to the tests to make it easier to observe any damage to them or any loss of fragments. Seventy cycles of 24 h each were carried out in each test under stable environmental conditions of $T = 20 \pm 5$ °C and RH = 30% $\pm$ 5. Three cubes of 40-mm edge were used in each test and for each consolidating material. The salt crystallization test was carried out using a solution of 14% Na$_2$SO$_4 \times 10$H$_2$O.

Ultrasonic measurements

The dynamic behavior and the degree of compactness of the stone during accelerated aging tests were evaluated by ultrasounds using a Panametrics HV Pulser/Receiver 5058PR coupled with a Tektronix TDS 3012B oscilloscope under controlled thermo-hygrometric conditions (T ~ 20 °C and RH ~ 35%), according to the ASTM D 2845-05 (2005). A couple of non-polarized piezoelectric transducers were used, with a frequency spectrum of 0.5 MHz. The measurements were performed on 3 cube samples per each treated stone (untreated and consolidated stones) in three perpendicular directions. We used a viscoelastic couplant (an ultrasound eco-gel) to ensure good coupling between the transducers and the stone surface. The transmission method was used and three measurements were taken for each orthogonal direction of the samples. The propagation velocities of the compression waves (V_p) were calculated with the following equation:

$$V_p = \frac{L_p}{T_p};$$

where V_p (in m/s) is the pulse-propagation velocity in m/s, L_p (in m) is the pulse-travel distance and T_p (in s) is the effective pulse-travel time.

Changes in the visual appearance and microtexture of the stone

The chromatic differences between untreated and treated samples were evaluated using a Konica Minolta CM-700d spectrophotometer equipped with a xenon lamp and diffuse reflectance geometry. The measurement conditions were an illumination diameter of 8 mm, specular component in SCI/SCE mode, and a wavelength range from 400 to 700 nm with an interval of 10 nm. The illuminant mode used in the taking of measurements was 8 . Four measurements were taken on each face of the samples according to UNE-EN 15886 (2011). The difference in color (ΔE^*_{ab*}) was calculated using the following equation:

$$\Delta E^*_{ab} = \sqrt{\left(\Delta L^*\right)^2 + \left(\Delta a^*\right)^2 + \left(\Delta b^*\right)^2}$$

where L^* (lightness) varies from 0 (black) to 100 (white), and a^* and b^* (chromatic parameters) vary from -60 to $+60$: a^* from red ($+a^*$) to green ($-a^*$), and b^* from yellow ($+b^*$) to blue ($-b^*$).

The changes in the microtexture of the samples were analyzed 1 month after the application of the consolidants. Analysis was conducted using a BRUKER field emission scanning electron microscope (FE-SEM), Leo-Gemini model, equipped with an EDX microanalysis system.

Drilling resistance

The drilling profiles offer a direct way to evaluate the action of the consolidant in depth, so enabling us to interpret the efficiency of the two treatments on the beige stone (Rodrigues et al. 2018). The test was carried out using a DRMS Cordless Drill (Sint Technology) equipped with a 5-mm diameter bit with a flat edge and a diamond-covered tip. The drilling conditions were rotation speed of 600 rpm, penetration rate of 10 mm/min, and hole depth of 5 mm. Tests were conducted on untreated samples and on treated samples 10 days after application of the consolidant.

Results and discussion

Hydric behavior

The results of the hydric tests and water vapor permeability are set out in Fig. 2. The untreated stones of NL and DAP treatments had similar hydric behavior, as reflected in the free water absorption and drying curves (Fig. 2a, b). The behavior of the NL-treated sample under free water absorption was similar to that of the non-consolidated stone (Fig. 2a), but samples treated with NL absorbed less water and reached visual saturation more quickly (3 h).

We noticed a few small differences in the drying process in that the treated samples took longer to dry (almost three times as long as the untreated samples). The behavior under free water absorption of the sample treated with DAP was very different in comparison to the untreated sample. In fact, the DAP consolidating treatment had a positive impact on the hydric behavior of the stones, resulting in a much longer water absorption time (10 h) (Fig. 2b). On the other hand, the treated sample took longer to dry (2 days), which might be a negative aspect for the durability of the stone. The pore system is responsible for the different drying speeds, as larger pores are the first to empty, while smaller pores remain full of water (Scherer 1990). Hence, it probably took longer for the treated stones to dry due to the fact that the pores had become smaller so causing the water to be retained longer inside the pore system which may affect the durability of the stone. A rapid drying of the stone surface would be ideal as it would reduce biological growth, a factor of particular importance for the beige stone from the Pasargadae WHS due to the fact that microorganisms have been identified as the main decay factor affecting this stone (Shekofteh et al. 2018).

The capillarity absorption curves for the untreated samples also show similar patterns (Fig. 2c, d), as in both samples, the water reached the top after 3 weeks in three stages (from the start to 5 h, from 5 h to 1 week, and from 1 to 3 weeks). NL treatment resulted in less water being absorbed by capillary uptake in comparison with the untreated sample, although the rate of water absorption by capillary uptake increased. In the treated samples, water uptake reached the first stage of absorption in 4 h, and the second stage in 3 days while the untreated samples reached the first stage of water uptake in 5 h and the second stage in 1 week. This shows that water uptake was faster after treatment with NL (Fig. 2c). The absorption of water by capillary uptake was also faster after treatment with DAP reaching the maximum in 5 days in comparison with the 3 weeks taken by the untreated samples (Fig. 2d). These findings contrast with some reports in which water absorption by capillarity was almost unaffected by DAP treatment (Yang et al. 2014). The capillarity absorption kinetics give us some idea of the degree of connectivity among pores and the total amount of absorbed water depends above all on the total volume of the pores accessible to water (Cnudde et al. 2008). The curves c and d for the NL and DAP treatments show that although less water was absorbed, the speed of absorption increased in comparison with the untreated samples. The fact that smaller pores fill faster than bigger pores suggests that the pores became smaller after the treatments (in particular DAP-treated samples) (Martys and Ferraris 1997). It also indicated that these treatments do not change the connectivity of the pores completely. This is an advantage because a small change in water transport properties will not cause incompatibility issues.

The water vapor permeability curves shown in Fig. 2e indicated that the transpirability (permeability to water vapor) of treated stone is only slightly influenced by the NL consolidant and that the DAP treatment decreased the transpirability of the stone more than the NL treatment (Fig. 2f). It is important for the stone to remain permeable to water vapor, in order to avoid any build-up of moisture and soluble salts at the interface between the treated area and the untreated stone below (Price and Doehne 2011). In this sense at least, NL performs better in that it does not impair the transpirability of the beige stone. These slight changes induced by the NL treatment indicate that the pore throats are still connected, which is a positive sign.

The porosity results of the hydric tests are summarized in Table 1. The mean open porosity of the beige stone is 4.56%. The open porosity of both treated samples was similar to that of the untreated sample, although the porosity of the sample increased slightly after DAP treatment. This slight increase is also obvious in free water absorption, as samples treated with DAP had absorbed a slightly larger amount of water at the end of the water absorption test (Fig. 2b, I). By contrast, the NL treatment decreased the open porosity slightly, a fact that is
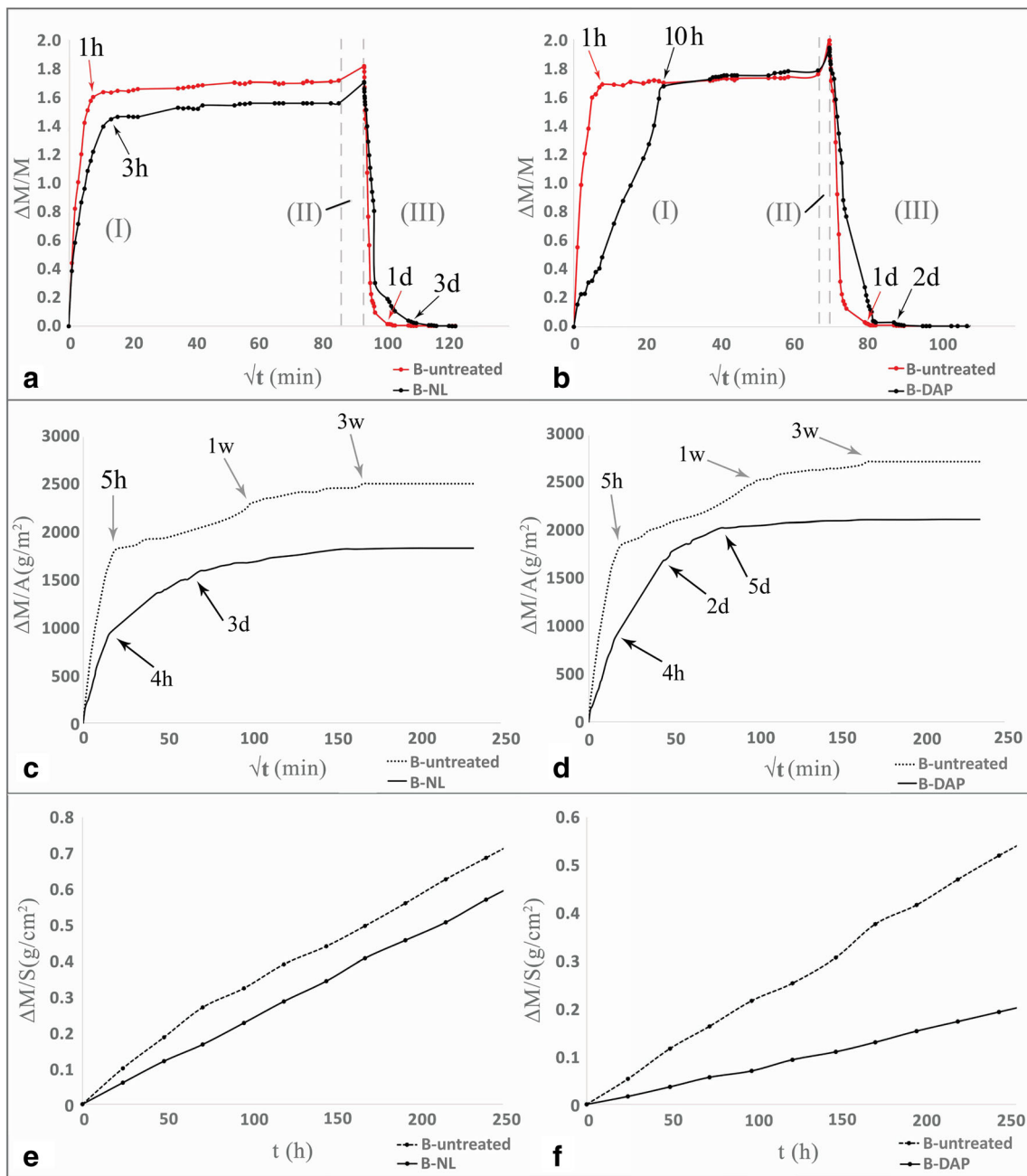
Fig. 2 **a** Free water absorption and drying curve for the untreated samples and the samples treated with NL. **b** Free water absorption and drying curve for the untreated samples and the samples treated with DAP; (I): free water absorption; (II): forced absorption; (III): water drying. Arrows indicate the time in hours (h), days (d), and weeks (w). **c** and **d** are the curves for the tests on water absorption by capillarity. **c** is the curve for the untreated samples and the stones treated with NL. **d** is the curve for the untreated samples and for those treated with DAP. **e** Water vapor permeability test on the untreated samples and those treated with NL. **f** Water vapor permeability test on the untreated samples and on those treated with DAP

reflected in the water absorption curves (Fig. 2a). However, it is important to bear in mind that the porosity values obtained from the hydric tests may not be reliable, in particular, in the case of a low porosity value such as that obtained for the beige stone. The changes in density are not significant because the layer of consolidating product is too thin to have significant effects on density.

Color changes

The lightness and chromic values for the untreated and treated samples are shown in Table 2. The L^* value in DAP-treated stones is higher than in those with treated with NL. DAP increased the lightness and yellowish index of the stone by almost 3 units, which can imply a slight chromatic change.

Table 1 Open porosity (P_{HT}, %), bulk (ρ_{Hb}), and skeletal (ρ_{Hsk}) density values obtained from the hydric tests (HT); NL refers to nanolime and DAP refers to dibasic ammonium phosphate

	P_{HT} %	ρ_{Hb}	ρ_{Hsk}
Untreated stone (NL)	4.40	2.51	2.63
NL treatment	4.27	2.50	2.61
Untreated stone (DAP)	4.72	2.44	2.56
DAP treatment	4.77	2.48	2.60

The difference in color after treatment with DAP (ΔE^{*}_{ab*} with about 4 units change) indicated that a difference in color between the treated and untreated stones could be detected by the human eye (Sasse and Snethlage 1996; Grossi et al. 2007). When ΔE^{*}_{ab*} is less than 3, the risk of incompatibility is almost 0, but when ΔE^{*}_{ab*} is between 3 and 5, the risk on the incompatibility rating scale rises to 5 (Benavente et al. 2003; Rodrigues and Grossi 2007). Therefore, the NL treatment has no significant effect on the color parameters of the stone, while DAP affects them slightly, in particular, by increasing the lightness and yellowness of the stone as previously reported by various researchers (Sassoni et al. 2011; Matteini et al. 2011). Considering that color changes of up to 5 on the incompatibility rating scale are commonly accepted after conservation work (Rodrigues and Grossi 2007), DAP may be regarded as a compatible treatment from an aesthetic point of view.

Superficial resistance

Figure 3 shows the drilling resistance of two treated stones and indicates that nanolime increases the superficial strength of the stones by about 2 N/mm and penetrates more than 6 mm inside the pores. Particles accumulate at around 2.2 mm beneath the surface (Fig. 3a). Treatment with DAP increased the superficial strength of beige stone in a similar way to the NL treatment, in particular, 5 mm from the surface. The particles accumulate about 3.1 mm beneath the surface (Fig. 3b), which is a good penetration depth given the low porosity of the beige stone.

Accelerated aging tests and ultrasonic measurements

Freeze-thaw

Figure 4 shows the results of the freeze-thaw tests and the weight changes in the samples over 70 cycles and the ultrasonic measurements taken every 5 cycles. We used ultrasonic measurements because the ultrasonic velocity can reveal the presence of cracks or fissures inside the stone that are otherwise impossible to observe or measure reliably (Vasanelli et al. 2017).

The freeze-thaw curve shows that microcracks occurred in the untreated samples from the 5th cycle onwards and that they expanded between the 15th and 20th cycle and then absorbed more water till the 30th cycle (Fig. 4a). It is interesting to notice that crack formation occurs later in samples treated with NL; the first microcrack began to develop after 20 cycles of the freeze-thaw test while the second microcrack appeared presumably after about 55 cycles. The ultrasonic wave propagation values for the untreated and treated samples, in total, indicate an increase (of almost 30%) in the compactness of the stone treated with NL (Fig. 4b). The appearance of cracks or fissures could not be observed clearly (Fig. 5a) but their presence could be deduced by ultrasonic velocity measurements, which recorded the strongest decrease (probably the main microcrack) at the 25th cycle, as shown by the weight loss in the freeze-thaw curve. After this, the ultrasound velocity remained almost unchanged until the end, while the untreated samples decreased again in the 60th cycle due to the formation of a microcrack. The main reason for the resistance of the beige stone to freeze-thaw damage is probably due to the absence of large pores in this stone (as manifested by the low porosity of the stone and the results obtained from its hydric properties) (Al-Omari et al. 2015). The compactness and durability of this stone are increased significantly after treatment with NL, even though it has good intrinsic resistance against freeze-thaw phenomena as can be seen at the Pasargadae WHS where there is an average of 55 days a year with freezing temperatures (Shekofteh et al. 2018).

Compared with the untreated samples (in which the first microcrack appeared in the 8th cycle), the weight of those treated with DAP remained unchanged up to the 23rd–25th cycles. These weight changes suggest that the DAP treatment
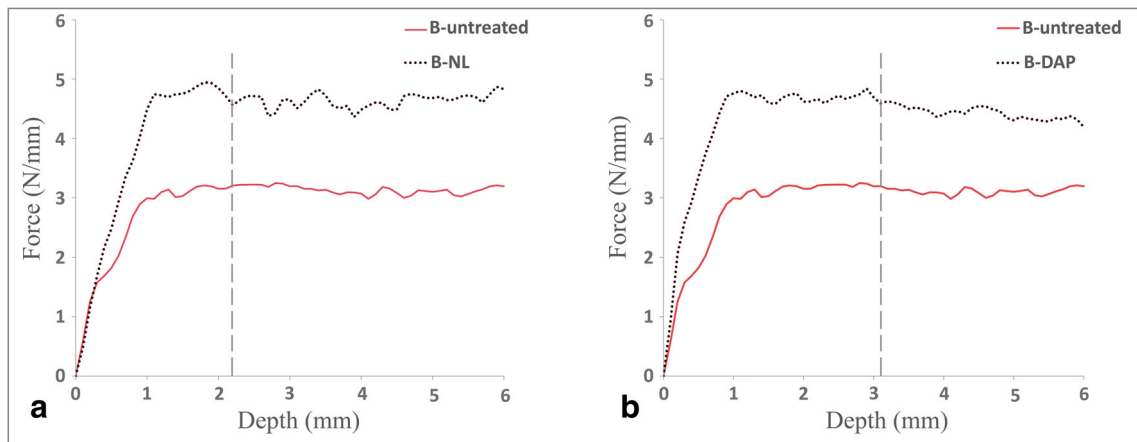
Table 2 Colorimetric measurements for the untreated and treated samples; NL refers to nanolime and DAP refers to dibasic ammonium phosphate

	L^{*}	a^{*}	b^{*}	
Untreated sample (NL)	84.05	1.53	5.83	
Untreated sample (DAP)	84.28	1.43	5.87	
	ΔL^{*}	Δa^{*}	Δb^{*}	ΔE^{*}_{ab*}
NL treatment	1.11	0.27	1.41	1.93
DAP treatment	3.31	0.87	3.20	4.03

Fig. 3 **a** Drilling resistance curve for untreated samples and samples treated with NL (B-NL). **b** Drilling resistance curve for untreated samples and samples treated with DAP (B-DAP); the dashed lines indicate the penetration depth of the accumulation of the consolidation material
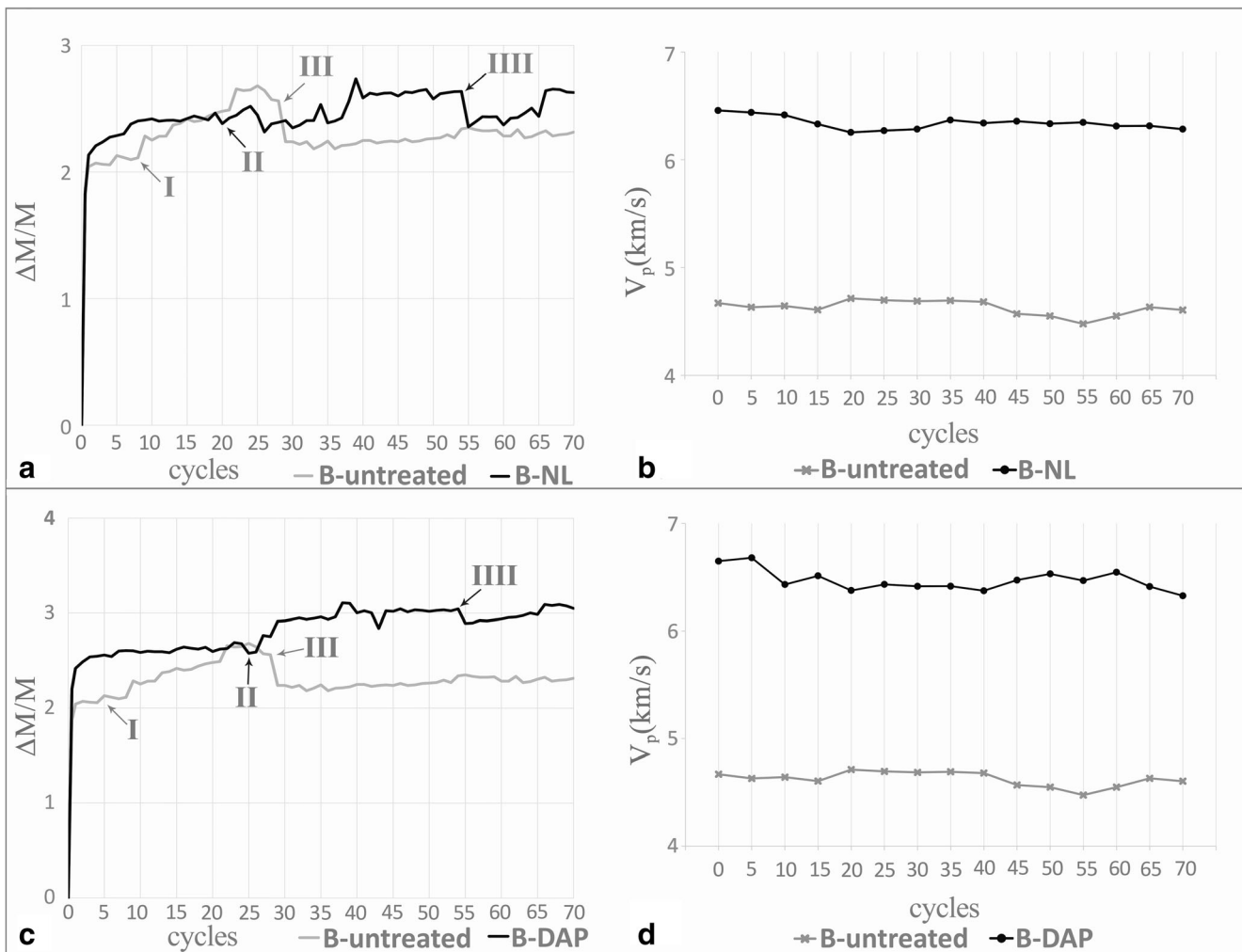

Fig. 4 **a** Weight loss evolution ($\Delta M/M$) during the freeze-thaw accelerated aging test on untreated samples and samples treated with the NL method; **b** P wave velocity (V_P, in km/s each 5 cycles) for untreated samples and samples treated with the NL method; **c** Weight loss ($\Delta M/M$) during the freeze-thaw accelerated aging test on untreated samples and samples treated with DAP. **d**

P wave velocity (V_P in km/s each 5 cycles) for untreated samples and samples treated with DAP; (I) first microcrack in untreated sample; (II) first main microcrack in treated sample; (III) second microcrack in untreated sample; (IIII) second main microcrack in treated sample
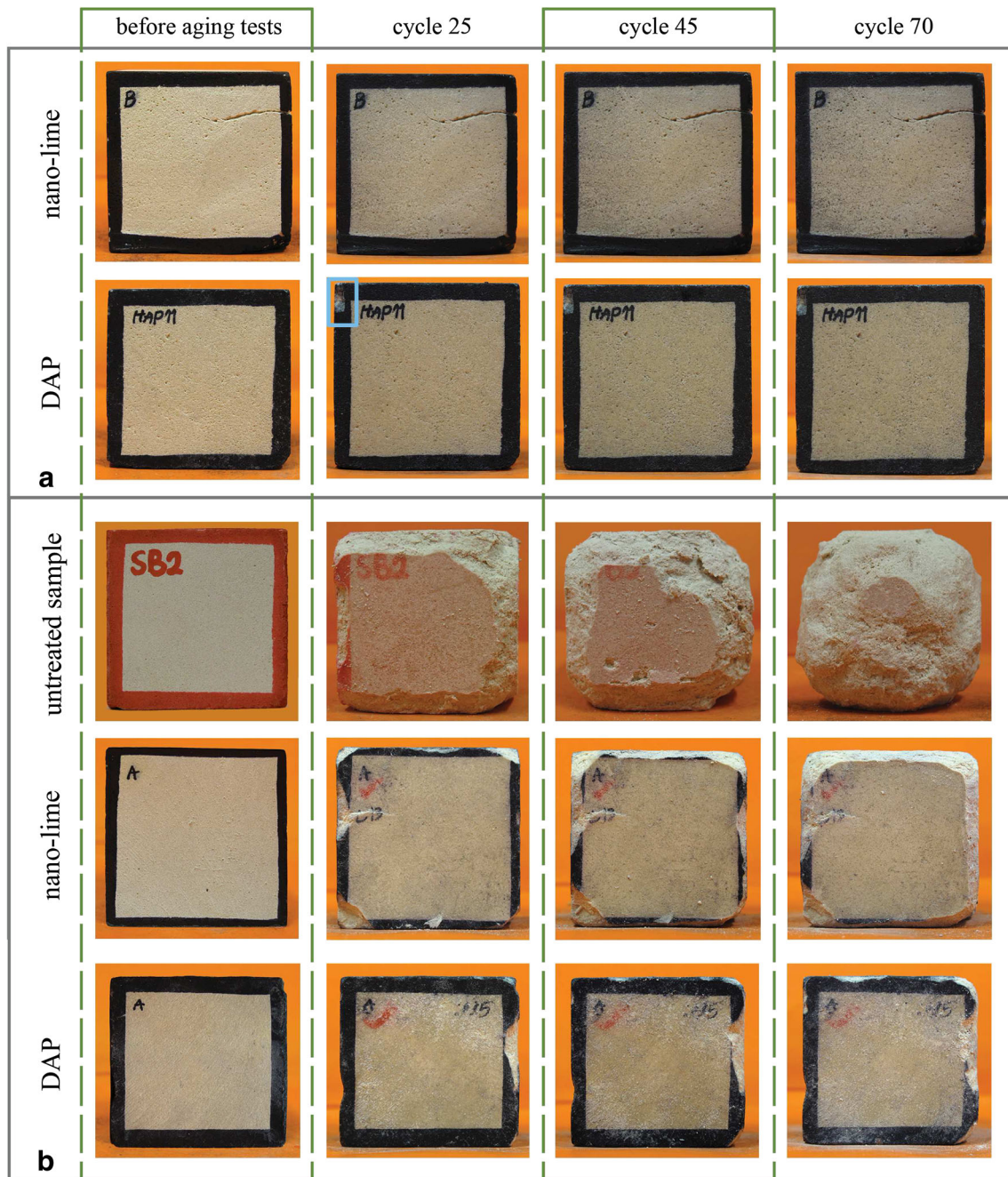
Fig. 5 (a) Visual appearance of the samples during the freeze-thaw test (70 cycles). The appearance remains unchanged except for a tiny fragment missing from one corner of the sample treated with DAP in the 25th cycle (the blue rectangle). We did not include the pictures of the untreated samples because there was no difference in appearance between untreated and treated samples. (b) Visual appearance of the samples during the salt crystallization test (70 cycles). The untreated samples suffered a great deal more than the treated samples and the DAP-treated sample resisted better than the sample treated with NL in terms of appearance

delayed the formation of the first microcrack by up to 17 cycles (Fig. 4c), while the ultrasound propagation velocity shows that the first microcrack developed in the 15th cycle (almost 10 cycles earlier than observed by the weight measurements) and another slight change in velocity was recorded in the 25th cycle (actually it lost a tiny fragment), remain unchanged until the 55th–60th cycles (Fig. 4d), as shown by the weight loss evolution in Fig. 4c and by the lost fragment in the 25th cycle (Fig. 5b). It is clear that NL produces a slight decrease in velocity during the freeze-thaw cycles, while DAP shows a bigger decrease from the beginning until the 25th cycle and then from the 60th to the 70th cycle. If the cycles had continued, it would presumably have suffered more with the formation of microcracks. Hence, the freeze-thaw cycles

indicated that the NL treatment improved the resistance of the beige stone to freezing more than the DAP treatment. This may be related to the reduction in porosity and the higher compatibility of nanolime crystals with the substrate due to the stress issues of CaP phases with $CaCO_3$.

Salt crystallization

Figure 6 shows the results of the salt crystallization test. As expected, this test caused more damage to the beige stone than the freeze-thaw test because it is more aggressive (Fig. 5a and b). As can be seen in Fig. 6a, even a small reduction of hydric properties and porosity has a significant influence on the resistance of the beige stone against salt crystallization, as shown by changes in both the appearance and the weight of the samples. This is because the resistance of the stone to salt crystallization is directly influenced by its porosity, water absorption, and capillarity uptake (Benavente et al. 2001; Beck and Al-Mukhtar 2010). The weight of the untreated samples decreased by around 20% over the 70 cycles, while the weight of the NL- and DAP-treated samples decreased by only 1% and less than 1%, respectively. The untreated samples also lost

some powdery fragments from their edges during the 70 test cycles. On visual inspection, no preferential orientation of the decay could be observed and the surface appeared slightly fragile and powdery. This behavior can be attributed to salt crystallization pressure and to the thenardite/mirabilite transition phase generated by sodium sulfate during immersion-drying cycles (Beck and Al-Mukhtar 2010). The surface of both treated samples remained intact (it was not fragile or powdery) and the DAP treatment lost some fragments from the edges (Fig. 5b).

The propagation of ultrasonic waves through the NL-treated samples showed an increase in compactness after consolidation (Fig. 6b). There was a reduction in the propagation velocity of treated samples above all over the first 15 cycles, although there was no evidence of this reduction in terms of weight loss ($\Delta M/M$). This means that the main microcracks in treated samples happened between the 10th and 15th cycles. By contrast, the velocity of the untreated samples fell gradually over the course of the test (70 cycles) and the main reduction happened in the first 5 cycles.

The ultrasonic wave propagations revealed a slightly larger increase in the compactness of the beige stone treated with
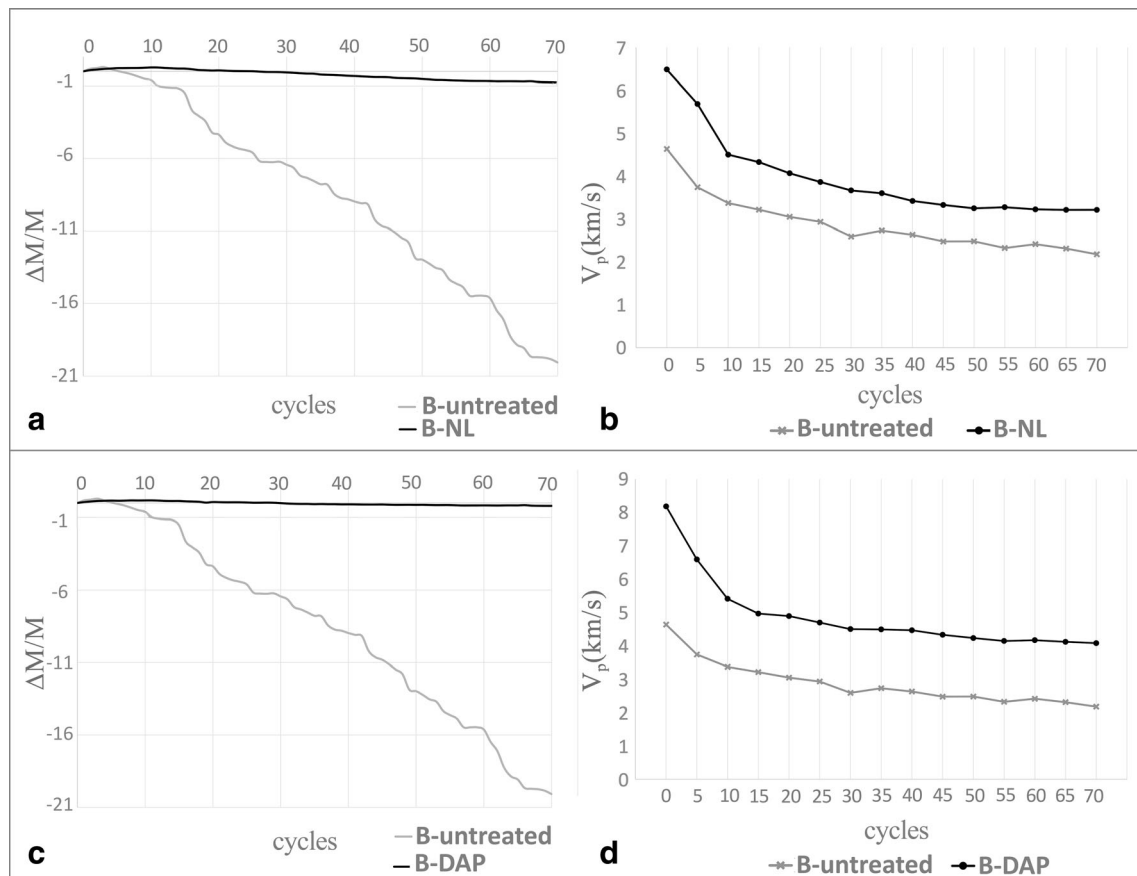

Fig. 6 a Weight loss evolution ($\Delta M/M$) during the salt crystallization test in untreated samples and samples treated with NL. b The P wave velocity (V_P, in km/s each 5 cycles) of both untreated samples and samples treated with NL. c weight loss evolution ($\Delta M/M$) during salt crystallization test in untreated samples and samples treated with DAP. d the P wave velocity (V_P, in km/s each 5 cycles) of both untreated samples and samples treated with DAP

DAP (about 44%) than when treated with NL, although the velocity results are similar, decreasing mainly during the first 15 cycles (Fig. 6d), after which it changed very little until the end of the test. We did not observe the formation of fragments during the first 15 salt crystallization cycles. This means that all fragment loss took place from the 15th cycle onwards and indicates that the first microcracks emerge early on without any external evidence to this effect, until fragments start falling off the edges (Fig. 5b). This may be due to improved pore space distribution in the treated samples compared with the untreated ones, so inducing different water transfer properties (permeability, capillarity, and water absorption) that affect the resistance of the stone against salt crystallization. This also proves that the unchanged appearance of the stone is not necessarily a sign that the salt has not affected the compactness of the stone.

Overall, DAP treatment increased the resistance of the beige stone against salt weathering slightly more than the NL treatment. The advantage of the DAP treatment is that it can be used even when the decayed stone has a gypsum crust (as an alternative source of calcium in the consolidation of the stone via the formation of calcium phosphates). It is also effective in the presence of salts because they do not interfere with the formation of calcium phosphates (Molina et al. 2017; Graziani et al. 2018). This indicates that DAP treatment can be used in altered carbonate stones, by pre-cleaning and consolidation in a single application in the case of gypsum crust via the reaction of DAP with gypsum as a source of calcium, so eliminating the sulfate at the same time. It can also be used for stones damaged by salt. Hence, DAP can be considered a suitable product for consolidating carbonate stone that has suffered salt damage. However, these advantages are not critical for the consolidation of stones that are not prone to salt damage and as we noticed, NL treatment resulted in similar resistance to salt crystallization, which given that the beige stone from the Pasargadae WHS does not suffer from salt crystallization (Shekofteh et al. 2018), means that both treatments are acceptable.

Microstructure observation

Microstructure observation by FE-SEM revealed that NL was homogeneously distributed across the sample and had given rise to phases with a similar morphology to those of the untreated limestone, so that it was hard to distinguish the treated surface from the untreated one. At higher magnification, the consolidating material could be distinguished thanks to the differences in the particle size of the phases (Fig. 7a). Nanoparticles from the nanolime treatment measure $\leq$ 300 nm under FE-SEM observation and tend to agglomerate within the pores of the stones. These nanoparticles are square to hexagonal in shape and are visible beside the calcite grains of the stone. The EDS analysis of the nanoparticles and the

grain indicated that Ca was the main element, which is related to the calcium carbonate. Figure 7b shows that the nanolime carbonation process continues in some calcite crystals, which indicates that the carbonation of nanolime takes longer than suggested in other previous research (Borsoi et al. 2016b; Otero et al. 2018).

Observation of the microstructure produced by DAP treatment revealed a homogeneous superficial film that includes diffused microcracks (Fig. 7c). EDS analysis identified Ca and P as the main elements, which may be related to the HAP phase, but it is important to bear in mind that distinguishing between different CaP phases on the basis of their different Ca/P ratio is challenging because CaP phase is often present in very small amounts and a conclusive identification is impossible due to the possible influence of the calcium-rich substrate on the Ca/P ratio (Sassoni 2018).

In fact, the cracks originate during drying due to shrinkage. To prevent cracking, lower concentrations of DAP (within the possible range of 0.1 to 3.7 M) are recommended, so leading to the formation of a thinner coating that is less prone to cracking (Graziani et al. 2016; Graziani et al. 2017b). With this in mind, we applied 1.0 M DAP with two brushstrokes (two thin films each formed at low DAP concentration), but after observing the SEM images, we quickly came to the conclusion that 1.0 M was not the right concentration of DAP for the beige stone. Recent studies have found that complete, uniform coverage can be ensured if 10 vol% ethanol is added to the DAP solution. Adding the ethanol reduces the concentration because the ethanol molecules weaken the hydration shell of the phosphate ions in solution (Sassoni et al. 2018). The pH can also affect the DAP concentration. This is because more PO_4^{3-} ions are expected to form from DAP dissociation at higher pH. The pH of the DAP solution can be increased by mixing with additives (e.g., $CaCl_2$) (Matteini 2008; Graziani et al. 2016; Molina et al. 2017). Calcium ions were added to the DAP solution because they offer two advantages: firstly, because they do not dissolve the substrate (the DAP treatment uses the added calcium ions to form HAP instead of calcium from the stone) and secondly, because they ensure faster, more complete coverage (Naidu and Scherer 2014). Other researchers studied two alternative methods to calcium ion addition: (1) pretreatment with limewater and (2) application of a limewater poultice after treatment with the DAP solution and drying (Graziani et al. 2017a; Sassoni et al. 2015). Eventually, modifications of this kind were rejected as they did not show significant benefits. The problem was that excessive growth of the coating caused diffused cracking in all cases, even when they attempted to reduce the DAP concentration by adding $CaCl_2$ in 1:1000 ratio to DAP and with 6 vol% ethanol to favor CaP formation (Sassoni et al. 2018). It is clear therefore that more research is required to produce a homogeneous superficial film without diffused microcracks, especially for open-air stone monuments such as the Pasargadae WHS.
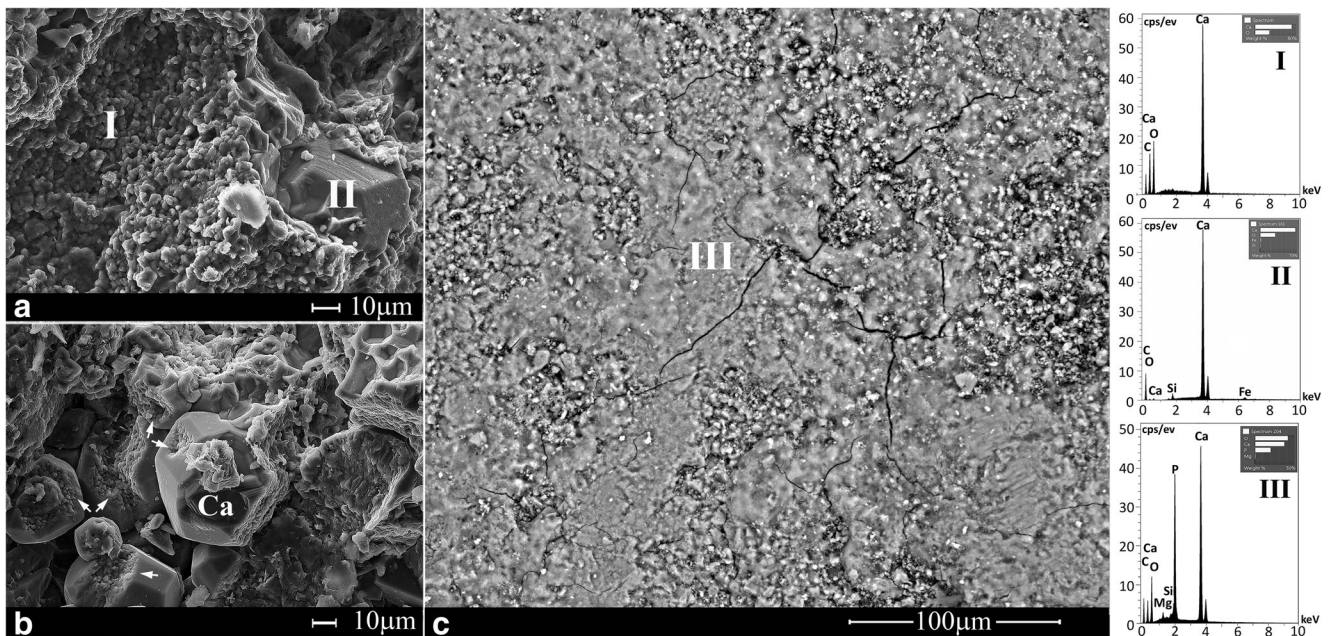
Fig. 7 SEM images of treated samples. **a** microstructure of the sample treated with NL, showing (I) the nanoparticles of the NL treatment beside (II) calcite crystals. **b** Magnification of the unfinished carbonation process, in which *Ca* highlights a calcite crystal and white arrows indicate uncompleted parts of the calcite crystals. **c** Superficial film of DAP on the beige stone includes diffused microcracks

In fact, if the pH is not adjusted, a 1.0 M DAP solution has a pH of 8.3. Under these conditions, only 0.003 M PO_4^{3-} ions are created from DAP. In addition to the formation of HAP, other CaP phases are expected to form within this pH range (Naidu and Scherer 2014; Eliaz and Metoki 2017). However, the formation of CaP phases improved hydric properties (in particular reduction of free water absorption) and mechanical strengthening, as revealed by increased micro-drilling resistance. Despite encouraging the formation of CaP phases which are highly resistant to dissolution in rain, DAP has an important drawback in terms of the formation of microcracks, which can allow rain to reach the substrate, so triggering dissolution. Some of the moisture that penetrates these microcracks is retained inside the layer of consolidant. This will presumably take longer to dry so favoring biological growth. The most important issues in relation to DAP treatment are therefore possible residues of unreacted DAP in the stone and the microcracks in the CaP film. These remain serious problems which require further research.

Conclusions

This study sought to evaluate the effectiveness of two common inorganic consolidating products when applied to the beige stone from the Pasargadae WHS (Iran): nanolime (NL) and dibasic ammonium phosphate (DAP). Both treatments had similar effects on the hydric properties of the stone, reducing free water absorption and capillarity. The main differences were that DAP treatment delayed water absorption more than NL, while NL reduced capillarity uptake more than DAP due to the reduction in porosity produced by NL treatment. Despite the predominant role of the capillary pores in water transfer, the DAP treatment reduced the water vapor permeability of the stone more than NL. The negative aspect of these treatments in terms of hydric behavior was that the treated samples dried more slowly than the untreated ones. The spectrophotometry data confirmed that DAP application changed the lightness and yellowish values, as manifested in an ΔE value of 4.03 between the untreated samples and those treated with DAP. This means that the human eye may notice differences in color between treated and untreated parts. However, in conservation works, color changes of less than 5 units are considered acceptable because these changes are unavoidable. We can therefore consider them compatible from an aesthetic point of view, although care should be taken, for example, when applying the product to brighter, whiter stones. The superficial resistance of both treatments increased by the same ratio (2 N/mm) and the penetration depths were 5–6 mm, which are acceptable given the low porosity of beige stone. Although NL-treated samples dried more slowly than DAP (1 day longer), NL was more resistant to the freeze-thaw test than DAP. For its part, DAP was more resistant to the salt crystallization test, at least in appearance. However, despite the unchanged appearance of both treated samples during the salt crystallization test, the reduction of ultrasound velocity revealed that they both suffered quite badly with salt crystallization from the start of the test up to the 15th cycle. This test

indicated that a slight reduction in the hydric properties and the porosity has a significant influence on the resistance of beige stone against salt crystallization, at least in appearance, although ultrasonic wave propagations indicated that the unchanged appearance of the stone does not necessarily mean that the salt had no impact on the stone. In total, both treatments improved the resistance of the beige stone to salt-induced decay more than its resistance to frost. Microstructure observation of the NL-treated sample showed the squared to hexagonal shapes of nanoparticles of carbonate calcium within the pores of the stones. This reduces the porosity of the stone. For its part, the DAP treatment formed a film of CaP phases that included diffused microcracks. The microstructure of DAP treatment might cause the samples to take longer to dry presumably due to the microcracks in the CaP film on the surface. In fact, water retention is an undesirable disadvantage of both treatments which may lead to decay processes because the moisture content is of crucial importance in terms of the resistance of the stone to frost damage. Hence, scaling can occur when moisture is present and the stone is exposed to natural freeze-thaw cycles. In addition to possible unreacted DAP, longer drying times can favor biological growth which, considering the problems with microorganisms in the beige stone of Pasargadae and the absence of salt as a decay factor (the decay problem that DAP treats best), leads us to conclude that DAP is not a suitable method for consolidating the beige stone from the Pasargadae WHS, in which the most important decay factor is microorganisms. In this case, nanolime would be the most suitable, most effective consolidation treatment.

References

Al-Omari A, Beck K, Brunetaud X, Török Á, Al-Mukhtar M (2015) Critical degree of saturation: a control factor of freeze–thaw damage of porous limestones at Castle of Chambord, France. Eng Geol 185: 71–80

Ambrosi M, Dei L, Giorgi R, Neto C, Baglioni P (2001) Colloidal particles of Ca (OH) 2: properties and applications to restoration of frescoes. Langmuir 17(14):4251–4255

ASTMD 2845-05 (2005) Standard method for laboratory determination of pulse velocities and ultrasonic elastic constants of rock. ASTM D2845-05

Barriuso BC, Botticelli G, Cuzman OA, Osticioli I, Tiano P, Matteini M (2017) Conservation of calcareous stone monuments: screening different diammonium phosphate based formulations for countering phototrophic colonization. J Cult Herit 27:97–106

Beck K, Al-Mukhtar M (2010) Evaluation of the compatibility of building limestones from salt crystallization experiments. Geol Soc Lond Spec Publ 333(1):111–118

Benavente D, del Cura MG, Bernabéu A, Ordóñez S (2001) Quantification of salt weathering in porous stones using an experimental continuous partial immersion method. Eng Geol 59(3–4): 313–325

Benavente D, Martínez-Verdú F, Bernabeu A et al (2003) Influence of surface roughness on color changes in building stones. Color research & application: endorsed by inter-society color council, the colour group (Great Britain), Canadian Society for Color, color science Association of Japan, Dutch Society for the Study of color, the Swedish colour Centre Foundation, colour Society of Australia. Centre Français de la Couleur 28(5):343–351

Boardman J (2000) Persia and the West: an archaeological investigation of the genesis of Achaemenid art. Thames & Hudson

Borsoi G, Tavares M, Veiga R, Silva AS (2012) Microstructural characterization of consolidant products for historical renders: an innovative nanostructured lime dispersion and a more traditional ethyl silicate limewater solution. Microsc Microanal 18(5):1181–1189

Borsoi G, Lubelli B, van Hees R, Veiga R, Silva AS (2016a) Optimization of nanolime solvent for the consolidation of coarse porous limestone. Applied Physics A 122(9):846

Borsoi G, Lubelli B, van Hees R, Veiga R, Silva AS (2016b) Understanding the transport of nanolime consolidants within Maastricht limestone. J Cult Herit 18:242–249

Borsoi G, Lubelli B, van Hees R, Veiga R, Silva AS (2017) Evaluation of the effectiveness and compatibility of nanolime consolidants with improved properties. Constr Build Mater 142:385–394

Carretti E, Dei L (2004) Physicochemical characterization of acrylic polymeric resins coating porous materials of artistic interest. Prog Org Coat 49(3):282–289

Chiantore O, Lazzari M (2001) Photo-oxidative stability of paraloid acrylic protective polymers. Polymer 42(1):17–27

Cnudde V, Dierick M, Vlassenbroeck J, Masschaele B, Lehmann E, Jacobs P, Van Hoorebeke L (2008) High-speed neutron radiography for monitoring the water absorption by capillarity in porous materials. Nucl Instrum Methods Phys Res Sect B 266(1):155–163

Daniele V, Taglieri G, Quaresima R (2008) The nanolimes in cultural heritage conservation: characterisation and analysis of the carbonatation process. J Cult Herit 9(3):294–301

Dei L, Salvadori B (2006) Nanotechnology in cultural heritage conservation: nanometric slaked lime saves architectonic and artistic surfaces from decay. J Cult Herit 7(2):110–115

Delgado Rodrigues J (2001) Consolidation of decayed stones. A delicate problem with few practical solutions. Historical Constructions, Guimarães. Portugal, pp 3–14

Eliaz N, Metoki N (2017) Calcium phosphate bioceramics: a review of their history, structure, properties, coating technologies and biomedical applications. Materials 10(4):334

Fidler J (2002) Lime treatments: an overview of lime watering and shelter coating of friable historic limestone masonry. English Heritage Res Trans 2:19–28

Franzoni E, Graziani G, Sassoni E, Bacilieri G, Griffa M, Lura P (2015a) Solvent-based ethyl silicate for stone consolidation: influence of the

application technique on penetration depth, efficacy and pore occlusion. Mater Struct 48(11):3503–3515

Franzoni E, Sassoni E, Graziani G (2015b) Brushing, poultice or immersion? The role of the application technique on the performance of a novel hydroxyapatite-based consolidating treatment for limestone. J Cult Herit 16(2):173–184

Giorgi R, Dei L, Baglioni P (2000) A new method for consolidating wall paintings based on dispersions of lime in alcohol. Stud Conserv 45(3):154–161

Graziani G, Sassoni E, Franzoni E (2015) Consolidation of porous carbonate stones by an innovative phosphate treatment: mechanical strengthening and physical-microstructural compatibility in comparison with TEOS-based treatments. Heritage Science 3(1):1

Graziani G, Sassoni E, Franzoni E, Scherer GW (2016) Hydroxyapatite coatings for marble protection: optimization of calcite covering and acid resistance. Appl Surf Sci 368:241–257

Graziani G, Sassoni E, Scherer GW, Franzoni E (2017a) Penetration depth and redistribution of an aqueous ammonium phosphate solution used for porous limestone consolidation by brushing and immersion. Constr Build Mater 148:571–578

Graziani G, Sassoni E, Scherer GW, Franzoni E (2017b) Resistance to simulated rain of hydroxyapatite-and calcium oxalate-based coatings for protection of marble against corrosion. Corros Sci 127:168–174

Graziani G, Sassoni E. Scherer G W, Franzoni E (2018) Phosphate-based treatments for consolidation of salt-bearing Globigerina limestone. In IOP Conference Series: Materials Science and Engineering (Vol 364, No 1, p 012082). IOP Publishing

Grossi CM, Brimblecombe P, Esbert RM, Alonso FJ (2007) Color changes in architectural limestones from pollution and cleaning. Color Res Appl 32:320–331

Hansen E, Doehne E, Fidler J, Larson J, Martin B, Matteini M, Rodriguez-Navarro C, Pardo ES, Price C, de Tagle A, Teutonico JM, Weiss N (2003) A review of selected inorganic consolidants and protective treatments for porous calcareous materials. Stud Conserv 48(sup1):13–25

López-Arce P, Gómez-Villalba LS, Martínez-Ramírez S, de Buergo MÁ, Fort R (2011) Influence of relative humidity on the carbonation of calcium hydroxide nanoparticles and the formation of calcium carbonate polymorphs. Powder Technol 205(1–3):263–269

Martys NS, Ferraris CF (1997) Capillary transport in mortars and concrete. Cem Concr Res 27(5):747–760

Matteini M (2008) Inorganic treatments for the consolidation and protection of stone artefacts. Conserv Sci Cultural Heritage 8(1):13–27

Matteini M, Rescic S, Fratini F, Botticelli G (2011) Ammonium phosphates as consolidating agents for carbonatic stone materials used in architecture and cultural heritage: preliminary research. Int J Archit Herit 5(6):717–736

Mohammadi P, Maghboli-Balasjin N (2014) Isolation and molecular identification of deteriorating fungi from Cyrus the Great tomb stones. Iran J Microbiol 6(5):361–370

Molina E, Rueda-Quero L, Benavente D, Burgos-Cara A, Ruiz-Agudo E, Cultrone G (2017) Gypsum crust as a source of calcium for the consolidation of carbonate stones using a calcium phosphate-based consolidant. Constr Build Mater 143:298–311

Naidu S, Scherer GW (2014) Nucleation, growth and evolution of calcium phosphate films on calcite. J Colloid Interface Sci 435:128–137

Natali I, Saladino ML, Andriulo F, Martino DC, Caponetti E, Carretti E, Dei L (2014) Consolidation and protection by nanolime: recent advances for the conservation of the graffiti, Carceri dello Steri Palermo and of the 18th century lunettes, SS. Giuda e Simone Cloister, Corniola (Empoli). J Cult Herit 15(2):151–158

NORMAL 29/88 (1988) Misura dell'indice di asciugamento (drying index). CNR-ICR, Rome, Italy

Otero J, Starinieri V, Charola AE (2018) Nanolime for the consolidation of lime mortars: a comparison of three available products. Constr Build Mater 181:394–407

Possenti E, Colombo C, Bersani D, Bertasa M, Botteon A, Conti C, Lottici PP, Realini M (2016) New insight on the interaction of diammonium hydrogenphosphate conservation treatment with carbonatic substrates: a multi-analytical approach. Microchem J 127:79–86

Price C A, Doehne E (2011) Stone conservation: an overview of current research. Getty Publications

Rodrigues JD, Grossi A (2007) Indicators and ratings for the compatibility assessment of conservation actions. J Cult Herit 8(1):32–43

Rodrigues JD, Pinto APF, Nogueira R, Gomes A (2018) Consolidation of lime mortars with ethyl silicate, nanolime and barium hydroxide. Effectiveness assessment with microdrilling data. J Cult Herit 29:43–53

Rodriguez-Navarro C, Suzuki A, Ruiz-Agudo E (2013) Alcohol dispersions of calcium hydroxide nanoparticles for stone conservation. Langmuir 29(36):11457–11470

Sasse HS, Snethlage R (1996) Methods for the evaluation of stone conservation treatments, in: Baer NS, Snethlage R (Eds.), Report of Dahlem workshop on saving our architectural heritage, Berlin, p 225

Sassoni E, Naidu S, Scherer GW (2011) The use of hydroxyapatite as a new inorganic consolidant for damaged carbonate stones. J Cult Herit 12(4):346–355

Sassoni E, Graziani G, Franzoni E (2015) Repair of sugaring marble by ammonium phosphate: comparison with ethyl silicate and ammonium oxalate and pilot application to historic artifact. Mater Des 88:1145–1157

Sassoni E, Graziani G, Franzoni E (2016) An innovative phosphate-based consolidant for limestone. Part 1: effectiveness and compatibility in comparison with ethyl silicate. Constr Build Mater 102:918–930

Sassoni E (2018) Hydroxyapatite and other calcium phosphates for the conservation of cultural heritage: a review. Materials 11(4):557

Sassoni E, Graziani G, Franzoni E, Scherer GW (2018) Calcium phosphate coatings for marble conservation: influence of ethanol and isopropanol addition to the precipitation medium on the coating microstructure and performance. Corros Sci 136:255–267

Scherer GW (1990) Theory of drying. J Am Ceram Soc 73(1):3–14

Shekofteh A, Molina E, Arizzi A, Cultrone G, Ahmadi H, Yazdi M (2016) Deterioration assessment of three types of limestones from Pasargadae World Heritage Site in Iran, 5th international conference YOCOCU 2016 (youth in conservation of cultural heritage), Madrid, Spain: 72-76

Shekofteh A, Molina E, Arizzi A, Cultrone G, Ahmadi H, Yazdi M (2018) Characterization and damage assessment of stones used in Pasargadae World Heritage Site, Achamenian period. Int J Archit Herit 13:521–536. https://doi.org/10.1080/15583058.2018.1436728

Shekofteh A (2018) Consolidation methodology for carbonate stones used in Pasargadae historic site, Doctoral dissertation, Art University of Isfahan, Iran

Sierra-Fernandez A, Gomez-Villalba LS, De la Rosa-García SC et al (2018) Inorganic nanomaterials for the consolidation and antifungal protection of stone heritage. In: In Advanced Materials for the Conservation of Stone. Springer, Cham, pp 125–149

Sohrabi M, Favero-Longo SE, Pérez-Ortega S, Ascaso C, Haghighat Z, Talebian MH, Fadaei H, de los Ríos A (2017) Lichen colonization and associated deterioration processes in Pasargadae, UNESCO world heritage site, Iran. Int Biodeterior Biodegradation 117:171–182

Song Y, Hahn HH, Hoffmann E (2002) The effect of carbonate on the precipitation of calcium phosphate. Environ Technol 23(2):207–215

Stronach D (1985) Pasargadae, in The Cambridge History of Iran. In: Gershevitch I (ed) the Median and Achaemenian periods, II edn. Cambridge University Press, Cambridge, pp 838–855

Tiano P (1995) Stone reinforcement by calcite crystal precipitation induced by organic matrix macromolecules. Stud Conserv 40(3):171–176

Tilia AB (1968) A study on the methods of working and restoring stone and on the parts left unfinished in Achaemenian architecture and sculpture. East and West 18(1/2):67–95

UNE-EN 1925 (2000) Natural stone test methods. Determination of water absorption coefficient by capillarity. In: AENOR. Madrid, Spain

UNE-EN 12370 (2001) Metodi di prova per pietre naturali. Determinazione della resistenza alla cristallizzazione dei sali. CNRICR, Rome, Italy

UNE-EN 1936 (2007) Natural stone test methods. Determination of real density and apparent density, and of total and open porosity. In: AENOR. Madrid, Spain

UNE-EN 13755 (2008) Natural stone test methods. Determination of water absorption at atmospheric pressure. In: AENOR. Madrid, Spain

UNE-EN 15803 (2010) Conservación del patrimonio cultural. Métodos de ensayo. Determinación de la permeabilidad al vapor de agua, AENOR, Madrid, Spain

UNE-EN 12371 (2011) Natural stone test methods. Determination of frost resistance. AENOR, Madrid, Spain

UNE-EN 15886 (2011) Conservation of cultural property. Test methods. Colour measurement of surfaces, AENOR, Madrid, Spain

van Hees R, Lubelli B, Nijland T, Bernar A (2014) Compatibility and performance criteria for nanolime consolidants. Proceedings of the 9th International Symposium on the Conservation of Monuments in the Mediterranean Basin- Monubasin, 3–5 June 2014. Ankara

Vasanelli E, Calia A, Luprano V, Micelli F (2017) Ultrasonic pulse velocity test for non-destructive investigations of historical masonries: an experimental study of the effect of frequency and applied load on the response of a limestone. Mater Struct 50(1):38

Wheeler G, Goins ES (2005) Alkoxysilanes and the consolidation of stone. Getty Publications, Los Angeles

Yang F, Liu Y, Zuo G, Wang X, Hua P, Ma Q, Dong G, Yue Y, Zhang B (2014) Hydroxyapatite conversion layer for the preservation of surface gypsification marble relics. Corros Sci 88:6–9

Zornoza-Indart A, López-Arce P, López-Polín L (2017) Durability of traditional and new nanoparticle based consolidating products for the treatment of archaeological stone tools: chert artifacts from Atapuerca sites (Burgos, Spain). J Cult Herit 24:9–21